Modeling of a continuous sewage sludge paddle dryer by coupling Markov chains with penetration theory

Mathieu Milhé, Martial Sauceau, Patricia Arlabosse

Modeling of a continuous sewage sludge paddle dryer by coupling Markov chains with penetration theory

M. Milhé*, M. Sauceau, P. Arlabosse

Université de Toulouse; Mines Albi; CNRS; Centre RAPSODEE, Campus Jarlard, F-81013 Albi, France

* Corresponding author: Tel +33563493052, mathieu.milhe@mines-albi.fr

Keywords: Sewage sludge; Paddle dryer; Markov chains; Penetration theory

Abstract

Sewage sludge can be dried in paddle dryers and turned into an interesting material for energetic valorization. This costly operation generally relies on manufacturer's know how and is not very flexible. Setting up a descriptive model of such dryers could lead to a better energy integration of this technology and make sludge drying more competitive by adjusting the operating conditions in order to reach the desired water content depending on subsequent applications. This paper presents the development of such a model adapted to a continuous pilot-scale sludge paddle dryer. The model combines sewage sludge flow description by means of a homogeneous Markov chain and drying kinetics thanks to the penetration theory, leading to the simulation of water content and temperature profiles along the dryer during steady-state operation. The principle of coupling these models is presented and the approach is validated against experimental data in various operating conditions. A parametric study emphasizes the crucial role of wall temperature and sludge residence time on the final water content, while stirring speed or sludge initial water content are less influent.

1. Introduction

Sewage sludge (SS) management is a matter of growing importance as its production keeps increasing with population growth and legislation evolution. Storage and hygiene issues, as well as landfilling limitation, contribute to make drying a necessary step in sewage sludge treatment and valorization [1]. Moreover, SS represents a promising feedstock for the waste to energy processes since it has a high organic content. Different technologies are being studied, or already implemented for managing this product alone or in combination with other wastes or feedstock. SS torrefaction [2] or pyrolysis [3–7] for materials and energy vectors production are actively studied; gasification also represents an interesting process for its valorization [8,9]. Nevertheless, these processes are highly energy-demanding even when operated with dry SS, and the high water content (w) of dewatered SS is a clear economical bottleneck for the development of such energetic valorization pathways. Indeed, at the outlet of a Waste Water Treatment Plant (WWTP), dewatered SS generally has $3 < w < 4.5\ kg/kg\ db$ (kg of water per kg of sludge on dry basis) depending on the dewatering technology as well as the different prior treatment steps. It is thus obvious that an efficient drying step is needed in order to make energetic valorization an interesting pathway for SS. Moreover, this drying step should be done in a flexible way, in order to adapt the water content to the minimal requirements of the different valorization pathways and reduce operating costs [10]. This reasoning excludes *de facto* the solar drying solution, which is more adapted to small- or medium-scale WWTPs, while thermal solutions (either direct or indirect processes) are more suitable for WWTPs operating for over 100,000 population equivalent.

However, rheological behavior description of such a product remains a scientific challenge. SS is a complex material whose behavior is not yet modeled by classical rheology particularly during drying when its water content decreases. Moreover its properties can vary according to numerous factors, including the type of physicochemical and biological wastewater

treatments, pre-conditioning and dewatering techniques used, or the period of the year [14,15]. CFD and classical mechanistic approaches for SS flow modeling are thus not applicable. From a process point of view, SS is a product difficult to handle, as it undergoes a transition from the initial pasty state corresponding to a typical dewatered sludge ($w \sim 3-4$ kg/kg db), to a so-called sticky state when it reaches $w \sim 1.5$ kg/kg db [11]. In this state, SS tends to form big lumps of material and is very difficult to mix efficiently: this results in dramatic increases in torque values required for maintaining the stirring action, which is potentially damageable for industrial contact dryers where moving equipment is involved [12]. For this reason, paddle dryers are recognized as well adapted tools for SS drying: thanks to the wedge-shaped paddles, the product undergoes high shearing stress and *in situ* clogging is avoided. Moreover, this kind of indirect dryer offers the advantages of compactness and low exhaust volumes [10]. In spite of the important number of installations functioning at an industrial scale, design and operation of paddle dryers mostly rely on manufacturers' know-how [13].

Few studies focused on the description of sludge drying in paddle dryers in continuous operation: while Arlabosse et al. [13] described drying kinetics along an industrial scale installation with a simple empirical model assuming plug flow of sludge, Tazaki et al. highlighted the importance of back-mixing, or recirculation, in such installations via a Residence Time Distribution (RTD) study [16]. They fitted their model of continuous stirred tank reactor (CSTR) in series to experimental results by considering adjustable recirculation coefficients between the different zones along the dryer. According to their results, obtained on an industrial-scale installation equipped with spiral disks, recirculation occurs mainly for $0.5 < w < 1.7$ kg/kg db, i.e. in the first part of the dryer they studied. It was then found to decrease in the second part of the dryer. This very interesting work cannot however be

directly transposed to paddle dryers, which have quite different stirrers design that probably results in a different mixing effect.

More recently, Charlou et al. developed a methodology for measuring experimental RTD with a good repeatability in a pilot-scale paddle dryer installation [17]. This study showed that water and dry solids have the same RTD, that is to say SS acts as a single phase during drying. Moreover the same authors showed that this RTD can be described by a Markov chain, where each paddle represents a continuous stirred tank reactor (CSTR) [18]. These CSTRs exchange sludge flows in both directions, resulting in recirculation between the reactors: this is characterized by a recirculation coefficient R representing the ratio of recirculated material to the overall throughput in the reactor calculated on a dry basis, as in Tazaki's work. This approach relies on the determination of transition probabilities between a cell and its neighbors during a given "transition time": SS flow is then considered as a time-discretized phenomenon [19]. The idea when representing the system by a Markov chain is having a flexible physically-based model that can be combined with a discretized heat-transfer model such as the penetration theory. However, there is yet no theory that could *a priori* lead to the estimation of R based on sludge water content. Hence, while in Tazaki's work, R was assumed to vary between the eleven zones studied and represented as much adjustable parameters, it was considered constant in Milhé's work [18]. The differences in scale and stirrer design of both experimental devices do not allow to judge of the respective pertinence of one or the other approach, all the more since all R values are not available in Tazaki's article, but rather four smoothed values.

The so-called penetration theory has been developed in the 80s for the description of heat transfer by conduction to agitated granular free flowing solids; it was later extended to the description of drying such agitated beds [20–22]. It was then successfully adapted to the drying of pasty products such as bentonite [23] and SS in batch lab-scale installations [24–

26]. This theory postulates that, in such systems, drying can be described by a series of static periods during which transient heat transfer and water evaporation occur, separated by instantaneous perfect macro-mixing of the bulk [21,22]. Such models give access to the calculation of an effective heat transfer coefficient between the heated wall and the wet solids, depending among others on SS water content and temperature. Since drying is considered as a succession of transient phenomena in this model, it is hardly compatible with a continuous flow model. On the other hand, its combination with a Markov chains-based flow model is appealing, provided both models can be simulated on a common time-scale. This paper is dedicated in a first part to the setup of the coupling of Markov chains and the penetration theory, for the description of a continuous pilot-scale paddle dryer during steady-state operation. This model is then validated with experimental water content profiles in different operating conditions and a parametric study is finally presented.

2. Material and methods

2.1 Continuous paddle dryer

The lab-scale pilot paddle dryer used in this work is represented in Figure 1; it has been described in previous works [17,27], so only its main features will be described here. It is a U-shaped dryer housing a single shaft, where the walls and the shaft are electrically heated. 18 paddles are regularly spaced on the shaft and heated by conduction. Dewatered SS is fed by a Moineau pump and the dried sludge is continuously weighed at the outlet of the dryer. Torque is also recorded, and its stability along with that of the outlet flow rate assesses a stationary operation. Once a steady state is reached and maintained for at least two hours, feeding and stirring are simultaneously stopped and sludge is sampled at nine different locations inside the dryer in order to obtain a water content profile along the dryer. The experimental data used for the model validation were obtained in the framework of a design of experiments, in which

overflow height, dryer slope, SS feeding flow rate and stirring speed were varied [28]. SS used in this experimental study was produced in the Albi municipal WWTP (France), operating for 60,000 population equivalent. Main characteristics for this sludge, which did not change significantly during the experimental campaign, can be found in [17].

2.2 Stochastic flow modeling: Markov chain

The Markov chain modeling of sludge flow has been described in another publication [18], but its main features are also recalled here. In a Markov chain with discrete time and discrete space of state, a property is distributed between *n* different states; the evolution of this distribution relies on an *n*-by-*n* matrix, which represents all the possible transitions from any state to every other. These transition probabilities are calculated for a given transition time: when these calculations do not change with time, the chain is said homogeneous.

The flow model considered here is illustrated in Figure 1, with the different dry sludge flows indicated. The different states in this system are the positions where an element of sludge can be found in the dryer: each one corresponds to the surroundings of a paddle. Each state, or cell, is assimilated to a Continuous Stirred Tank Reactor (CSTR). The matrix of transition probabilities of this system then represents the ability of sludge to flow between the different cells. These transition probabilities are calculated according to three parameters describing the flows and hold-up of each cell, namely $R(i)$ the recirculation coefficient from cell $i+1$ to cell i, Hu the dry solids hold-up in the dryer, and Δt the transition time, and two operating parameters, Q_{ds} the dry solids flow rate and n. With the assumptions that the hold-up is the same in each cell, the probability to remain in the same cell $P_{i,i}$ during Δt is:

$$P_{i,i} = 1 - \frac{\Delta t}{\tau_{ci}} \qquad \text{Eq. 1}$$

Where τ_{ci} is the geometric residence time in the cell i taking into account all the recirculation flows calculated as in Eq. 2 for $2 < i < n$ and as in Eq. 3 for $i = 1$.

$$\tau_{ci} = \frac{Hu}{n} \frac{1}{Q_{ds}[1+R(i-1)+R(i)]} \quad \text{Eq. 2}$$

$$\tau_{c1} = \frac{\left(\frac{Hu}{n}+Q_{ds}\Delta t\right)}{Q_{ds}[1+R(i)]} \quad \text{Eq. 3}$$

The sum of the different transition probabilities for a given cell must be equal to 1: this is the condition of normalization for Markov chains, expressed in Eq. 4 where $P_{j,i}$ is the probability to move from a cell i to a cell j.

$$\forall\, i,\ \sum_j P_{j,i} = 1 \quad \text{Eq. 4}$$

Moreover, it is also supposed that sludge can only move to neighboring cells during Δt. Hence, the backwards ($P_{i-1,i}$) and forwards ($P_{i+1,i}$) transition probabilities from the cell i are easily deduced as in Eq. 5 and Eq. 6. It is obvious that in the first cell no backwards transition is possible since the dryer has closed boundaries: $P_{0,1}$ does not exist, and $R(0) = 0$. In the same fashion, since the n+1th cell is the outlet of the dryer, $P_{n+1,n+1} = 1$ and $R(n) = 0$.

$$P_{i-1,i} = \frac{R(i-1)}{[1+R(i-1)+R(i)]}\left(1 - P_{i,i}\right) \quad (1 < i < n) \quad \text{Eq. 5}$$

$$P_{i+1,i} = \frac{1+R(i)}{[1+R(i-1)+R(i)]}\left(1 - P_{i,i}\right) \quad (1 < i < n) \quad \text{Eq. 6}$$

All the transition probabilities $P_{j,i}$ constitute the matrix of transition probabilities M, which is tridiagonal in this case. In the situation of a continuous sludge feeding with a dry solids feeding rate Q_{ds}, let S be a column vector of n+1 scalars representing dry sludge distribution in the system: its evolution during Δt is calculated according to Eq. 7, where S_{in} is the column vector representing sludge feeding as in Eq. 8.

$$S(t + \Delta t) = M \times (S(t) + S_{in}) \quad \text{Eq. 7}$$

$$S_{in} = [(Q_{ds} \times \Delta t)\ 0\ 0\ \cdots 0]' \quad \text{Eq. 8}$$

At this point, the calculation of the $P_{j,i}$ should be discussed. In a first version of this model used for Residence Time Distribution (RTD) simulations [29], it was calculated according to

Eq. 9. However, as highlighted by Tamir [30], this expression was first introduced without proof by Fan et al. [31], indicating that only small values of Δt should be used. However, this approach does not allow closing properly a mass balance on the system, even if the condition of normality is actually respected.

$$P_{i,i} = e^{\left(-\frac{\Delta t}{\tau_{ci}}\right)} \qquad \text{Eq. 9}$$

Figure 2 illustrates the evolution of the total hold-up in the system during a simulation with constant flow rate imposed in the first cell and initial hold-up Hu_{ini}. Simulations were carried out with different values of the ratio $\Delta t/\tau_c$, using Eq. 9 or Eq. 1 for the calculations of the matrix M. Since the system is supposed to be at steady-state, the quantity of dry solids in the system should remain equal to Hu_{ini}, the value for which the transition probabilities are computed. It is obvious that when using Eq. 9, some material accumulates in the system, as illustrated by the increase in the value of $Hu(t)/Hu_{ini}$; moreover, the higher the $\Delta t/\tau_c$ ratio, the greater the deviation. On the contrary, the results were similar for any value of the $\Delta t/\tau_c$ ratio taken between 0 and 1 with Eq. 1 so only one is represented here. However this ratio should not be higher than one because the model loses its physical sense and the simulations diverge. Using Eq. 1 or Eq. 9 is equivalent for small values of Δt because $\lim_{x\to 0} e^{-x} = 1 - x$, so the previous results obtained in [29] still hold. However, the use of Eq. 1 is recommended since it is based on a mass balance. Moreover in the following, implementing the penetration theory along with this flow model will imply working with Δt values higher by an order of magnitude than in the previous works, as will be presented in section 2.4.

2.3 Heat transfer and drying: penetration theory

The so-called penetration theory considers the continuous contact drying of an agitated wet granular packing as a succession of static periods and of instantaneous mixing of the bulk. The particles bed is considered as a saturated mono-dispersed packing of spheres. During the

static periods, transient propagation of a drying front occurs from the dryer wall to the free surface of the bulk, while the mixing step is supposed to be ideal; the duration of the static periods is classically noted t_r [22,32]. This theory has been extensively described in several configurations and will not be repeated here.

It has been proven efficient in describing drying kinetics of SS in batch lab-scale installations under different operating conditions: partial air vacuum [26], atmospheric air pressure [25] or superheated steam atmosphere where there is no mass transfer resistance in the gaseous phase [24]. This work is concerned with the latter configuration, in which it has been shown that the limiting mechanism during SS drying is the contact resistance between the heated walls and the biggest particles. The characteristic particle diameter is then set at 1.15 mm in a first attempt as in [24]. The methods for sludge physical properties determination such as thermal conductivity of dry sludge or total heat of vaporization are described in previous publications on the subject [13,24]. Since similar values were obtained by two different teams [24,26], they will be employed in this work and are gathered in Table 1.

Table 1: Physical properties of dry SS and steam considered in this work

Dry sludge physical properties						
Particle size (*m*)	*Particle rugosity* (-)	*Surface covering factor*	*Thermal conductivity* (*W*/(*m.K*))	*Specific heat* (*J*/(*kg.K*))	*Surface roughness* (*m*)	*Bulk density* (kg/m^3)
$1.15.10^{-3}$	$1.5.10^{-5}$	0.8	0.13	1 400	15.10^{-6}	700
Steam physical properties						
Thermal conductivity at 100°C (*W*/(*m.K*))	*Specific heat at 100°C* (*J*/(*kg.K*))	*Pressure* (*bar*)	*Latent heat of vaporization* (*J*/*kg*)			
0.025	2 077	1.01325	2 257 000			

With the assumption that there is no heat transfer between wet and dry particles during mixing, the position of a drying front during a transient fictitious period is obtained by solving Fourier's equation with Neumann's solution for a constant wall temperature. The transient drying rate obtained is then averaged during t_r. t_r is related to the mixing number N_{mix}

according to Eq. 10, where N is the rotation speed of the stirrer. N_{mix} was defined in the first publications on the subject by an empirical correlation based on the Froude number Fr as in Eq. 11, where a and b are coefficients bound to the type of dryer studied, D is the diameter of the dryer and g the gravitational constant [33].

$$t_r = {N_{mix}}/{N} \qquad \text{Eq. 10}$$

$$N_{mix} = aFr^b = a\left(\frac{(2\pi N)^2 D}{g}\right)^b \qquad \text{Eq. 11}$$

As emphasized in [34], the correlation obtained by Mollekopf and presented in [33] may not be valid with any products or stirrer designs: the determination of an appropriate value for N_{mix} is thus not straightforward. In the latter reference, the authors deduced a = 9 and b = 0.05 from experimental studies on two paddle dryers of different scales. These correlations have been used satisfactorily in previous studies concerned with the application of the penetration theory to SS drying in batch installations [24,26]. However, in another study on a twin-shaft paddle dryer operated batch-wise, the authors preferred to identify N_{mix} by optimization between experimental and predicted results [25]. For a stirring speed of 17 rpm, this approach lead them to a value of N_{mix} = 8.5 while using Eq. 11 would have given a value of N_{mix} = 6.5. Since these values are quite close, and given the weak influence of N_{mix} on the drying rate on such a narrow range [24], it was decided to keep estimating N_{mix} with Mollekopf's correlation in this study.

2.4 Contact area estimation

Another important parameter of this theory is the heated area in contact with sludge. If it can be straightforward in batch installations, provided that all the heating area remains covered by sludge during drying, it may vary along a continuous dryer not only due to SS water content change, but also to the local sludge volume in each cell. For this reason, a contact area is computed for each cell in the Markov model, depending on the amount of sludge in this cell

and on its water content. Each cell is considered as a half-cylinder topped by a rectangular volume of the same height; the rotor bearing the paddles is situated on the same symmetrical axis than the half cylinder. The area corresponding to the side walls and the rotor is taken into account for heat transfer, since these elements are heated and their surface temperature is assumed constant. The cell structure and this contact area ae illustrated in Figure 3. The paddles are only heated by conduction and actually act as "coolers". Temperature profiles were simulated on COMSOL© and indicate that they are responsible for less than 15% of the total heat flux in the first part of the dryer, where the driving force is the most important (lowest SS temperature and highest water content resulting in high heat transfer coefficient). The paddle contact area was thus not taken into account in this work. The volume of sludge in each cell is computed after each transition; the contact area is then deduced from geometric considerations, assuming that sludge acts as a free-flowing material.

As long as SS can be considered as a continuum, i.e. before granulation occurs, bulk specific density of sludge ρ_{wet} is supposed to be the weighted arithmetic mean between that of water ρ_w and dry sludge true density ρ_{ds} according to Eq. 12. This hypothesis is supported by the fact that during sludge drying, an ideal shrinkage is usually observed, so the volume of water evaporated corresponds to the change in volume observed in a sludge sample due to drying as long as SS matrix is not rigid [35]. The values for sludge bulk density estimated this way agree well with that measured with classical soil tests in [36].

$$\rho_{wet} = \frac{w+1}{\frac{w}{\rho_w}+\frac{1}{\rho_{ds}}} \qquad \text{Eq. 12}$$

A limit water content $w_{crit} = 1.5\,\text{kg/kg db}$ is defined based on experimental observations, corresponding to a bulk density value of $\rho_{wet,crit} = 1160\ kg/m^3$. For $w < w_{crit}$, granulation occurs due to the combined effects of matrix hardening and high shearing due to the paddles: it is no longer possible to consider sludge as a continuum. Sludge bulk density is then

supposed to decrease linearly from $\rho_{wet,crit}$ down to $\rho_{dry} = 700\ kg/m^3$, which is the dry bulk density obtained for totally dried sludge based on experimental observations. The evolution of wet sludge bulk density with water content considered in this study is illustrated in Figure 4.

2.5 Coupling algorithm: time discretization and convergence

Coupling the flow and heat transfer models is easily done when both models are set up on the same characteristic time. The following algorithm is used in order to determine SS water content and temperature profiles at steady state for a given set of operating conditions:

- The dryer is initially filled with sludge at 100°C and $w = 4\ \mathrm{kg/kg\ db}$;
- Water vaporization occurs in each cell according to the penetration theory during a fictitious period Δt after which water content and bulk temperatures are re-computed in each cell;
- The amounts of dry SS and water due to the continuous feed are added to the first cell, along with the corresponding enthalpies: water content and bulk temperature of the cell are re-computed;
- The contents of the different cells are redistributed along and out of the dryer according to the Markov chain, due to the macro-mixing occurring after Δt; water content and bulk temperatures are then re-computed in each cell;
- These steps are repeated a number of times representing at least twice the dry solids mean residence time;
- Iterations are stopped when a steady-state is reached: such a steady state would be assessed by the stability of water contents and sludge temperatures in the cells for a certain time.

As observed earlier, the choice of the transition time Δt has no effect on the flow pattern as described by a Markov chain, so its value can be set according to the penetration model. In this study, this transition time is thus calculated according to Eq. 10 and only depends on the

stirring speed chosen. A simple relationship between bulk temperature T_b and enthalpies of dry solid and liquid phases is considered, since no phase change is involved during the feeding and mixing steps. By considering the reference enthalpy equal to 0 at 0°C and constant specific heats for both water Cp_w and dry sludge Cp_{DS} Eq. 13 gives the bulk temperature in any cell, with the amount of dry sludge m_{DS} or water m_w in the cell in kg and SS specific enthalpy h_b in J/kg.

$$T_b = \frac{h_b}{m_{DS}Cp_{DS}+m_wCp_w} \qquad \text{Eq. 13}$$

Some other simplifications are considered in this study:

- If SS temperature is lower than 100°C in a cell because of fresh sludge feeding or mixing with cells below 100°C, the heat flux necessary to heat up the sludge in this cell to 100°C is subtracted to the heat flux computed with the penetration theory.
- An empirical correlation (Eq. 14, where Lv is the latent heat of water vaporization at normal pressure) for the total heat of sorption was derived from calorimetry experiments and takes into account the hygroscopicity of SS (see [37]). However, due to its exponential form, this relationship results in unrealistically high values of total heat of sorption for the lowest water content: the total heat of sorption is thus limited to 3.6 MJ/kg, corresponding to the experimental value obtained for $w = 0.05$ kg/ kg db. Without this limitation, sludge temperature rises to very high values when its water content is close to 0.

  $$\Delta H_{tot} = L_v + 7.94.10^6 e^{(-25.5w)} \qquad \text{Eq. 14}$$

- Convective heat flux from the superheated steam atmosphere is not taken into account in this study. Even though steam used as a sweeping gas is generated at a temperature of 160°C, its temperature inside the dryer fluctuates around 120°C due to punctual heat losses and low flow rate (1.1 kg/h). Moreover its speed is very low, and the flow

of steam generated by the drying sludge itself is close to or superior to that of sweeping gas depending on operating conditions.

Finally, two criteria have to be matched for exiting the algorithm: water content and temperatures stability are evaluated as in Eq. 15, where *S* is a vector of dimension *n* standing for any of these variables, over a duration t_{stab}. This duration was set at one third of the average dry solids residence time in the dryer in order to avoid stopping of the algorithm due to slow evolution of the system between two iterations. $\varepsilon = 10^{-2}$ was found to be a good value combining results accuracy with relatively low computer time.

$$\frac{\|S(t)-S(t-t_{stab})\|}{\|S(t)\|} < \varepsilon \qquad \text{Eq. 15}$$

Several initial conditions were tested: the simulated dryer was filled at the beginning with sludge at 100°C and $1 < w < 5$ kg/kg db. All these initializations lead to the same steady-state solution in comparable number of iterations.

3. Results and discussion

3.1 Experimental results

A series of experiments were carried out with varying operating conditions, which are gathered in Table 2: *Q* is the sludge inlet flow rate on a wet basis, w_{in} the initial water content and *N* the dryer stirring speed. The dry solids Mean Residence Time (MRT), as calculated by Eq. 16, are also indicated. Wall temperature was set at 160°C for all experiments.

$$MRT = \frac{w_{in}Q}{Hu} \qquad \text{Eq. 16}$$

Table 2: Operating conditions

Experiment	**Operating conditions**				
	Q (*kg/h wb*)	*N* (*rpm*)	*Hu* (*kg*)	w_{in} (*kg/kg db*)	*MRT* (*h*)
A	3	31.5	0.80	3.65	1.24
B	3	31.5	1.79	3.65	2.77
C	4	21	3.00	3.80	3.60

Sludge water content profiles for the three experiments of Table 2 are illustrated in Figure 5. Overall, the higher the dry solids MRT, the lower the water content, particularly in the second half of the dryer. In experiments B and C however, the last samples show comparable water contents and the two last samples of experiment A show an increase in water content where one would await a decrease. These discrepancies illustrate the difficulty linked to product sampling in a continuous reactor. Nevertheless, the trends are logical, and in the following more attention will be paid to the general evolution of the simulated profiles rather than sludge water content at the final sampling point.

Another observation is that there seems to be two zones in the dryer: in the first one, water content decreases faster for all experiments, down to a water content of ca. 1.5 kg /kg db for exp. A and below 1 kg/kg db for the others. After this phase, a slower decrease in water content is observed and the drying fluxes look rather comparable between the experiments. This is emphasized in Figure 6, where the corresponding drying fluxes in kg H_2O/h are illustrated. They are calculated as in Eq. 17 after the experimental water content profiles, where $\dot{w}_i$ is the drying flux at sampling position *i* and w_i is the corresponding water content.

$$\dot{w}_i = \frac{Q}{1+w_{in}}(w_{i-1} - w_i) \qquad \text{Eq. 17}$$

Two zones are clearly distinguishable: in the first half of the dryer, mean drying rates are close to 0.5 kg/h, while in the second half they are close to 0.1 kg/h for all experiments. The discrepancies are important however, so the mean drying rates were calculated over the first four samples and the five last ones: they are gathered in Table 3. Drying rates in the first part of the dryer seem to increase linearly with dry sludge MRT. However, the differences in

drying rates in the first part do not explain completely the differences observed in terms of water content reached in the middle of the dryer. More insight can be obtained on these results by simulating them as is presented in the next part.

Table 3: Median water content and mean drying rates for the three experiments

	Water content at dryer middle (kg/kg db)	Mean drying flux (kg H_2O/h)	
		First half	*Second half*
Exp. A	1.24	0.36	0.08
Exp. B	0.60	0.47	0.08
Exp. C	0.55	0.67	0.09

3.2 Comparison of experimental and simulated results

For the following simulations, the same parameters as in Table 2 are applied to the model for the different simulations presented hereafter. Following previous work in which optimization of a RTD model lead to *R* values comprised between 2 and 6 [18], the recirculation coefficient was set to a value of $R = 4$. Simulations results are compared with experimental data for each experiment in Figure 7, for water content and drying flux profiles. The simulated drying fluxes were calculated every two model cells so as to be comparable with the experimental ones, based on nine sampling points. The model offers overall a satisfactory agreement with water content profiles from all experiments, in spite of an overestimation of the initial drying rates.

Simulated drying fluxes are also in qualitative agreement with experimental values, even though the latter are very scattered, which makes it difficult to go further in the analysis. It is interesting to see that in spite of the non-deterministic approach in modeling and strong hypotheses, SS drying behavior is well predicted in varying operating conditions by the model without any specific optimization procedure. Nevertheless, the simulated profiles are smoother and more monotonous than the experimental ones, so there is no clear difference between the two halves of the dryer. This could be due to the assumption of a constant

recirculation coefficient. Indeed, sludge flow properties vary strongly during drying, and it is expected that the behavior of pasty sludge in the first half of the dryer might be quite different from that of granular sludge in the second half, as is suggested by the experimental results. However, there is no scientific base for quantifying these differences, hence the choice of a constant *R* value in the model.

Krischer curves were plotted from the simulation data and are illustrated in Figure 8. The model allows estimating drying rates per unit area, so the different simulations can be compared even though the degree of filling of the dryer varied from an experiment to another. Drying rates are equivalent for experiments A and B, and slightly lower for experiment C. This is in agreement with the penetration theory, in which the shorter the contact times, the higher the heat transfer coefficients. In this case, the stirring speed was lower for experiment C, which resulted in a lower mixing number N_{mix} and a higher characteristic time t_r, while the wall temperature was the same. This trend is also observed in batch contact drying installations [24,32]. In the first cells, depending on operating conditions, SS temperature can be below 100°C due to fresh sludge feeding, so the drying rate is null. However, the water content is still below that of fresh SS since the model postulates that recirculation occurs between neighboring cells.

Evolution of SS temperature with respect to its water content is illustrated in Figure 9 for the three simulations. The rise in temperature observed for water contents under 1 kg/kg is typical for contact drying of particles beds. In the first model cells, SS temperature is below 100°C due to fresh sludge feeding, corresponding to the points where the drying rate was null in Figure 8. However, such information is not available experimentally and it is not possible to verify if SS temperature is actually lower than 100°C in the first zone of the dryer.

3.3 Parametric study

A parametric study was conducted in order to check some parameters influences on the results. Drying temperature, assimilated to the dryer wall temperature T_{wall}, Q_{in}, N and w_{in} were considered as operating parameters; the model sensibility to R was also studied. Common parameters values to all the simulations are gathered in Table 4: a constant dry solids hold up *Hu* was considered for all the simulations.

Table 4: Common parameters to the different simulations in the parametric study

Q_{in} (*kg/h*)	w_{in} (*kg/kg db*)	T_{wall} (*°C*)	N (*rpm*)	*Hu* (*kg ds*)	R (-)
5	4	160	30	2	4

- *Wall temperature*

Simulations were run with wall temperatures T_{wall} varying from 140 to 180°C. The resulting water content profiles, illustrated in Figure 10, show a logical trend: the higher T_{wall}, the more efficient the drying operation. The differences are greater in the second part of the dryer than at the beginning, even though the heat transfer coefficients decrease with decreasing SS water content. With the set of operating conditions chosen, the outlet water content ranges from 0.5 kg/kg at 180°C to 2.1 kg/kg at 140°C.

- *Inlet SS flow rate*

Simulations were run with Q_{in} varying from 3 to 7 kg/h. The resulting water content profiles are illustrated in Figure 11. Since *Hu* value remains the same, increasing Q_{in} is equivalent to decreasing sludge MRT. In this range of inlet flow rate, SS outlet water content increases from 0.1 to 2 kg/kg db. As previously, the difference is more marked in the end of the dryer than in the beginning. MRT was previously experimentally identified as a critical parameter for SS drying performance in paddle dryers [28].

- *Stirring speed*

Simulations were run with stirring speeds N varying from 10 to 50 rpm: the resulting water content profiles are illustrated in Figure 12. Combining Eq. 10 and 11, one obtains $t_r \propto N^{-0.9}$ for paddle dryers: N is thus more influent on t_r, and hence on the time-averaged heat

transfer coefficients from wall to SS bed, for small values. In the configuration of the pilot-scale installation considered here, the range of values studied leads to t_r values varying from 43 s down to 10 s with increasing N. The influence of N is weaker than the previous parameters: for these simulations, outlet SS water content was comprised between 1.2 and 1.4 kg/kg ds. This result is coherent with the existence of a critical resting time, below which drying rates do not increase with stirring speed [24,33]. This is to be related with the fact that the contact resistance between the wall and the first layer of particles does not depend on N, while the penetration resistance depends on the duration of the resting time t_r.

- *Inlet SS water content*

Simulations were run with SS initial water contents w_{in} varying from 3 to 5 kg H_2O/kg ds: the resulting water content profiles are illustrated in Figure 13. Contrary to first parameters studied, the differences between the simulations appear to decline along the dryer: even though the inlet water contents range from 3 to 5 kg/kg ds, at the outlet of the dryer they range from 0.95 to 1.4 kg/kg ds only. Actually, when considering a constant wet SS inlet flow rate, increasing SS initial water content is equivalent to increasing water flow rate and decreasing dry solids flow rate in the dryer. This results in a greater MRT, which leads to a more intense drying operation. This balance between increased inlet water content and increased MRT leads to small differences in the final water content, even though the initial water contents are very different. This observation should not be generalized to any full-scale installation however, since in the present model the contact area between sludge and heated walls also depends on water content. Industrial installations running at full capacity are characterized by constant contact areas.

- *Recirculation coefficient*

Simulations were run with varying values of the recirculation coefficient R, from 1 to 12: the resulting water content profiles are illustrated in Figure 14. Overall, the profiles are steeper

for the lowest values of R and more homogeneous for the higher values. Actually, increasing R comes back to considering the dryer as a CSTR, so the trend observed in this figure would lead to a constant SS water content along the dryer, with an important initial drying rate. On the contrary, with $R \to 0$, the model is closer to a series of CSTRs, so the dryer behavior will be closer to that of a plug flow reactor, with a continually decreasing drying rate. This parameter being purely numerical, these trends can only be used for model analysis and improvement. Qualitatively, if the agreement between model and experiments can be judged satisfying, it is clear that a constant recirculation coefficient between the cells is neither plausible nor represents the observations accurately. It is tempting to relate the two zones experimentally observed with high and low drying fluxes, in the first and second half of the dryer respectively, to zones with different values of R. Indeed, a lower initial R value would better describe the initial steep part of water content profiles; moreover, since SS seems to have a better flowability in granular state, corresponding to the dryer second part, than in pasty state in the first part. Such an approach would however have its drawbacks, since only optimization procedures could help deciding which R values would be suitable. Moreover, one should be aware that other model assumptions could be discussed in order to get a more physically sound model: for example, the assumption of a constant hold-up along the dryer, or that of a constant particle diameter during drying. These are strong hypotheses: however, working with different ones would also require either optimization procedures or developing new experimental approaches that go beyond the scope of this paper.

3.4 Model discussion

In the present version, the model was built to describe a single shaft paddle dryer and is not readily usable for a full-scale installation characterization. Particularly, it is based on the knowledge of the dry solids hold-up in the installation and the contact area is deduced from it at each calculation. Scale-up would require several steps in its development:

- The validity of the model flow based on Markov chains should be tested on larger-scale installations, particularly regarding the effect of several shafts on SS RTD,
- Heat transfer and drying rates computations should be carried out on the basis of an already known contact area between SS and heated walls (i.e. a pre-determined SS volume) and not on an arbitrary SS amount in each cell. This point implies working with non-homogeneous Markov chains, in which transition probabilities depend on the state of the system: indeed, with the assumption of a fixed SS volume in each cell, the amount of dry solids in each cell depends on its water content, and so does the calculation of the matrix *M*.
- A better accuracy could be obtained with the knowledge of the evolution of particle size distribution with the extent of drying. This important parameter is indeed decreasing in granular state due to comminution, as already observed for china clay [23].
- On a more fundamental level, there is a missing link between SS water content and temperature and its rheology, that could help relate SS state and its flow properties, particularly regarding the parameter *R*.

4. Conclusion

Paddle dryers are widely used for SS or other pasty products drying, but are operated based on empirical knowledge. A model was developed for the description of continuous SS drying in a single-shaft pilot paddle dryer in steady-state operation. The model combines SS flow description by means of a homogeneous Markov chain and heat transfer and drying kinetics thanks to the penetration theory. The principle of coupling these models is presented and the approach is validated against experimental data in various operating conditions.

A parametric study confirmed the strong influence of operating parameters such as wall temperature and inlet SS flow rate; on the contrary, stirring speed showed almost no influence in the range tested, while SS initial water content only had a limited influence on the outlet water content. Finally, the recirculation coefficient was shown to have a quite weak influence on outlet water content in the present configuration, but its role must be better understood for scaling-up purposes. This represents one of the few adjustments that would be required in order to adapt this model to full-scale installations description: its evolution towards a fixed-contact area configuration would make it a powerful tool for industrial installations study and optimization.

References

[1] D. Fytili, A. Zabaniotou, Utilization of sewage sludge in EU application of old and new methods--A review, Renew. Sustain. Energy Rev. 12 (2008) 116–140.

[2] M. Atienza-Martínez, I. Fonts, J. Ábrego, J. Ceamanos, G. Gea, Sewage sludge torrefaction in a fluidized bed reactor, Chem. Eng. J. 222 (2013) 534–545. doi:10.1016/j.cej.2013.02.075.

[3] E. Agrafioti, G. Bouras, D. Kalderis, E. Diamadopoulos, Biochar production by sewage sludge pyrolysis, J. Anal. Appl. Pyrolysis. 101 (2013) 72–78. doi:10.1016/j.jaap.2013.02.010.

[4] I. Fonts, M. Azuara, G. Gea, M.B. Murillo, Study of the pyrolysis liquids obtained from different sewage sludge, J. Anal. Appl. Pyrolysis. 85 (2009) 184–191. doi:10.1016/j.jaap.2008.11.003.

[5] Y. Cao, A. Pawłowski, Sewage sludge-to-energy approaches based on anaerobic digestion and pyrolysis: Brief overview and energy efficiency assessment, Renew. Sustain. Energy Rev. 16 (2012) 1657–1665. doi:10.1016/j.rser.2011.12.014.

[6] I. Fonts, G. Gea, M. Azuara, J. Ábrego, J. Arauzo, Sewage sludge pyrolysis for liquid production: A review, Renew. Sustain. Energy Rev. 16 (2012) 2781–2805. doi:10.1016/j.rser.2012.02.070.

[7] J. Ábrego, J.L. Sánchez, J. Arauzo, I. Fonts, N. Gil-Lalaguna, M. Atienza-Martínez, Technical and Energetic Assessment of a Three-Stage Thermochemical Treatment for Sewage Sludge, Energy Fuels. 27 (2013) 1026–1034. doi:10.1021/ef3018095.

[8] M. Dogru, A. Midilli, C.R. Howarth, Gasification of sewage sludge using a throated downdraft gasifier and uncertainty analysis, Fuel Process. Technol. 75 (2002) 55–82. doi:10.1016/S0378-3820(01)00234-X.

[9] N. Gil-Lalaguna, J.L. Sánchez, M.B. Murillo, V. Ruiz, G. Gea, Air-steam gasification of char derived from sewage sludge pyrolysis. Comparison with the gasification of sewage sludge, Fuel. 129 (2014) 147–155. doi:10.1016/j.fuel.2014.03.059.

[10] P. Arlabosse, J.-H. Ferrasse, D. Lecomte, M. Crine, Y. Dumont, A. Léonard, Efficient Sludge Thermal Processing: From Drying to Thermal Valorization, in: E. Tsotsas, A.S. Mujumdar (Eds.), Mod. Dry. Technol., Wiley-VCH Verlag GmbH & Co. KGaA, 2011: pp. 295–329. http://onlinelibrary.wiley.com/doi/10.1002/9783527631681.ch8/summary (accessed February 19, 2014).
[11] N. Ratkovich, W. Horn, F.P. Helmus, S. Rosenberger, W. Naessens, I. Nopens, et al., Activated sludge rheology: A critical review on data collection and modelling, Water Res. 47 (2013) 463–482. doi:10.1016/j.watres.2012.11.021.
[12] N. Eshtiaghi, F. Markis, S.D. Yap, J.-C. Baudez, P. Slatter, Rheological characterisation of municipal sludge: A review, Water Res. 47 (2013) 5493–5510. doi:10.1016/j.watres.2013.07.001.
[13] T. Kudra, Sticky Region in Drying: Definition and Identification, Dry. Technol. 21 (2003) 1457–1469. doi:10.1081/DRT-120024678.
[14] A. Ferrasse, J., H. P..., Heat, momentum, and mass transfer measurements in indirect agitated sludge dryer, Dry. Technol. 20 (2002) 749–769. doi:10.1081/DRT-120003755.
[15] P. Arlabosse, S. Chavez, D. Lecomte, Method for Thermal Design of Paddle Dryers: Application to Municipal Sewage Sludge, Dry. Technol. 22 (2004) 2375–2393. doi:10.1081/DRT-200040041.
[16] M. Tazaki, H. Tsuno, M. Takaoka, K. Shimizu, Modeling of Sludge Behavior in a Steam Dryer, Dry. Technol. 29 (2011) 1748–1757. doi:10.1080/07373937.2011.602811.
[17] C. Charlou, M. Milhé, M. Sauceau, P. Arlabosse, A new methodology for measurement of sludge residence time distribution in a paddle dryer using X-ray fluorescence analysis, Water Res. 69 (2015) 1–8. doi:10.1016/j.watres.2014.11.005.
[18] M. Milhé, C. Charlou, M. Sauceau, P. Arlabosse, Modeling of Sewage Sludge Flow in a Continuous Paddle Dryer, Dry. Technol. 0 (2014) null. doi:10.1080/07373937.2014.982252.
[19] H. Berthiaux, V. Mizonov, Applications of Markov Chains in Particulate Process Engineering: A Review, Can. J. Chem. Eng. 82 (2004) 1143–1168. doi:10.1002/cjce.5450820602.
[20] E.U. Schlünder, Heat transfer to packed and stirred beds from the surface of immersed bodies, Chem. Eng. Process. Process Intensif. 18 (1984) 31–53. doi:10.1016/0255-2701(84)85007-2.
[21] E. Tsotsas, E.U. Schlünder, Contact drying of mechanically agitated particulate material in the presence of inert gas, Chem. Eng. Process. Process Intensif. 20 (1986) 277–285. doi:10.1016/0255-2701(86)80021-6.
[22] E.U.S. E Tsotsas, Vacuum contact drying of free flowing mechanically agitated multigranular packings, Chem. Eng. Process. Process Intensif. (1986) 339–349. doi:10.1016/0255-2701(86)80012-5.
[23] A. Dittler, T. Bamberger, D. Gehrmann, E.-U. Schlünder, Measurement and simulation of the vacuum contact drying of pastes in a LIST-type kneader drier, Chem. Eng. Process. Process Intensif. 36 (1997) 301–308. doi:10.1016/S0255-2701(97)00004-4.
[24] P. Arlabosse, T. Chitu, Identification of the Limiting Mechanism in Contact Drying of Agitated Sewage Sludge, Dry. Technol. 25 (2007) 557–567. doi:10.1080/07373930701226955.
[25] W.-Y. Deng, J.-H. Yan, X.-D. Li, F. Wang, S.-Y. Lu, Y. Chi, et al., Measurement and simulation of the contact drying of sewage sludge in a Nara-type paddle dryer, Chem. Eng. Sci. 64 (2009) 5117–5124. doi:10.1016/j.ces.2009.08.015.
[26] J.-H. Yan, W.-Y. Deng, X.-D. Li, F. Wang, Y. Chi, S.-Y. Lu, et al., Experimental and Theoretical Study of Agitated Contact Drying of Sewage Sludge under Partial Vacuum Conditions, Dry. Technol. 27 (2009) 787–796. doi:10.1080/07373930902900911.

[27] C. Charlou, M. Sauceau, P. Arlabosse, Characterisation of Residence Time Distribution in a Continuous Paddle Dryer, J. Residuals Sci. Technol. 10 (2013) 117–125.
[28] M. Milhé, M. Sauceau, P. Arlabosse, Determination of dry sludge hold-up in a continuous paddle dryer, in: Izmir, Turkey, 2014.
[29] M. Milhé, C. Charlou, M. Sauceau, P. Arlabosse, Modeling of sewage sludge flow in a continuous paddle dryer, Dry. Technol. Accept. Publ. (n.d.).
[30] A. Tamir, Chapter 4 - Application of Markov chains in chemical reactors, in: A. Tamir (Ed.), Appl. Markov Chains Chem. Eng., Elsevier Science B.V., Amsterdam, 1998: pp. 334–497. http://www.sciencedirect.com/science/article/pii/B9780444823564500067.
[31] L.T. Fan, J.R. Too, R. Nassar, Stochastic simulation of residence time distribution curves, Chem. Eng. Sci. 40 (1985) 1743–1749. doi:10.1016/0009-2509(85)80036-1.
[32] E. Tsotsas, E.U. Schlünder, Contact drying of mechanically agitated particulate material in the presence of inert gas, Chem. Eng. Process. Process Intensif. 20 (1986) 277–285. doi:10.1016/0255-2701(86)80021-6.
[33] E.-U. Schlünder, N. Mollekopf, Vacuum contact drying of free flowing mechanically agitated particulate material, Chem. Eng. Process. Process Intensif. 18 (1984) 93–111. doi:10.1016/0255-2701(84)85012-6.
[34] E. Tsotsas, M. Kwapinska, G. Saage, Modeling of Contact Dryers, Dry. Technol. 25 (2007) 1377–1391. doi:10.1080/07373930701439079.
[35] T. Ruiz, C. Wisniewski, Correlation between dewatering and hydro-textural characteristics of sewage sludge during drying, Sep. Purif. Technol. 61 (2008) 204–210. doi:10.1016/j.seppur.2007.07.054.
[36] B.C. O'Kelly, Mechanical properties of dewatered sewage sludge, Waste Manag. 25 (2005) 47–52. doi:10.1016/j.wasman.2004.08.003.
[37] J.-H. Ferrasse, D. Lecomte, Simultaneous heat-flow differential calorimetry and thermogravimetry for fast determination of sorption isotherms and heat of sorption in environmental or food engineering, Chem. Eng. Sci. 59 (2004) 1365–1376. doi:10.1016/j.ces.2004.01.002.

Figure captions

Figure 1: Scheme of the lab-scale continuous paddle dryer studied (a), structure of the model considered for the Markov flow model where n is the number of paddles/cells, Qds the dry solids flowrate, R the recirculation coefficient, some transition probabilities are indicated (b)

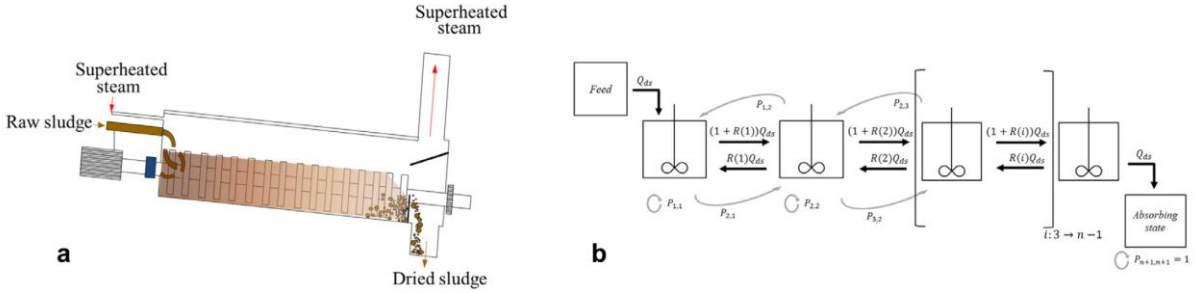

Figure 2: Evolution of the total dry solids hold-up during a simulation with the probabilities $P_{i,i}$ calculated according to Eq. 1 with $\Delta t/\tau_c = 0.2$ (solid line) and Eq. 9 (dashed line: $\Delta t/\tau_c = 0.2$; dotted line: $\Delta t/\tau_c = 0.1$; dashed-dot line: $\Delta t/\tau_c = 0.01$)

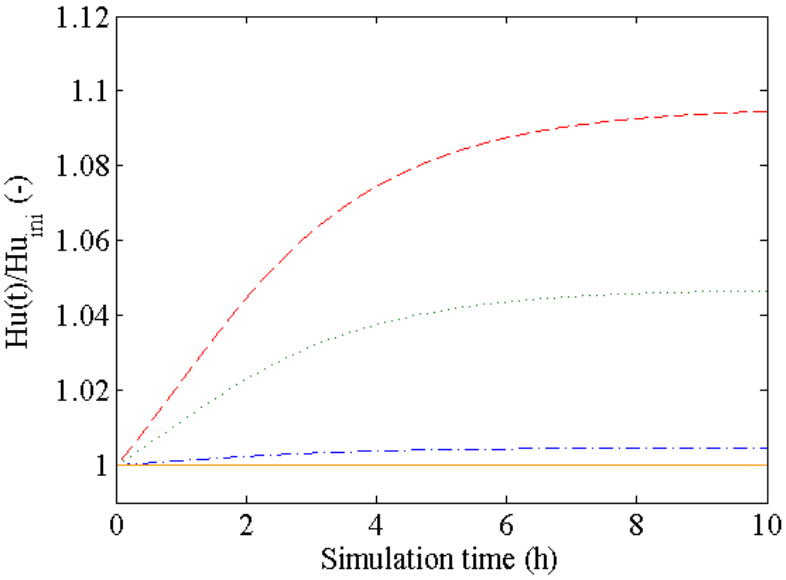

Figure 3: Illustration of a cell structure and the contact area taken into account for heat transfer (in green shade)

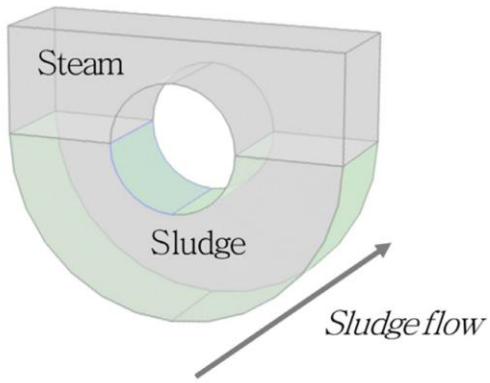

Figure 4: Evolution of sludge bulk density with water content, the discontinuity marks the beginning of granulation

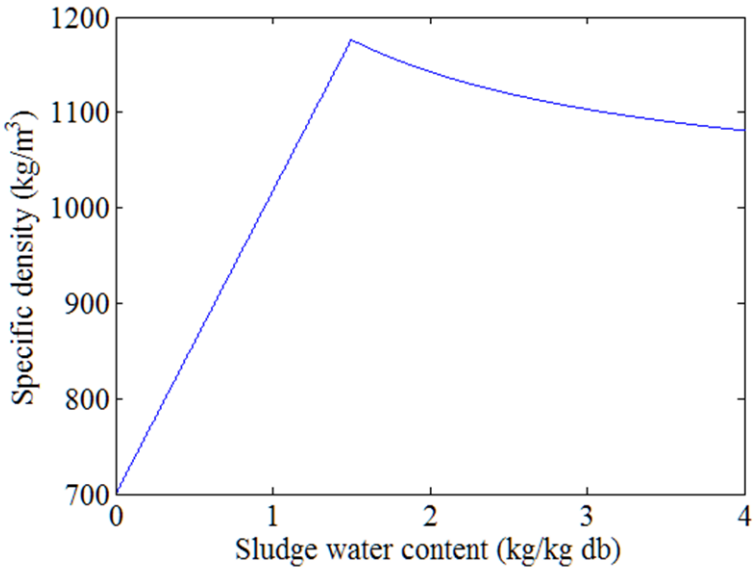

Figure 5: Experimental water content profiles (● Exp. A; ■ Exp. B; ▲ Exp. C)

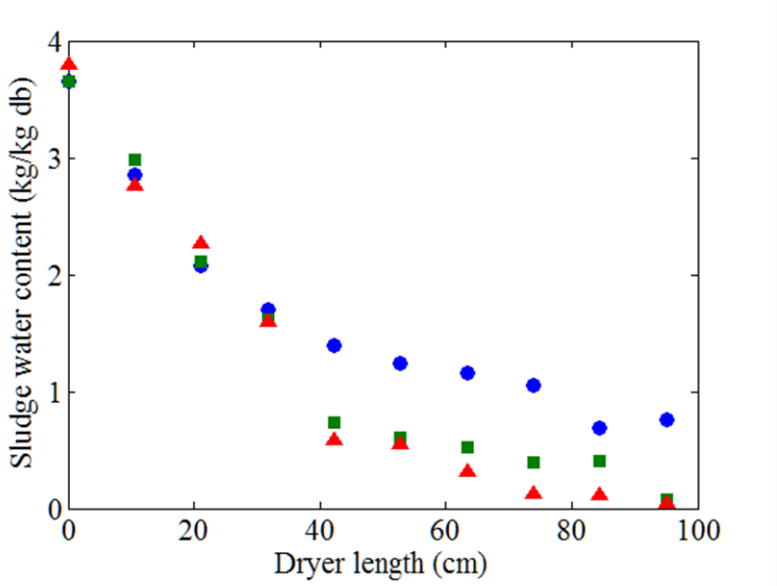

Figure 6: Experimental drying flux profiles (● Exp. A; ■ Exp. B; ▲ Exp. C)

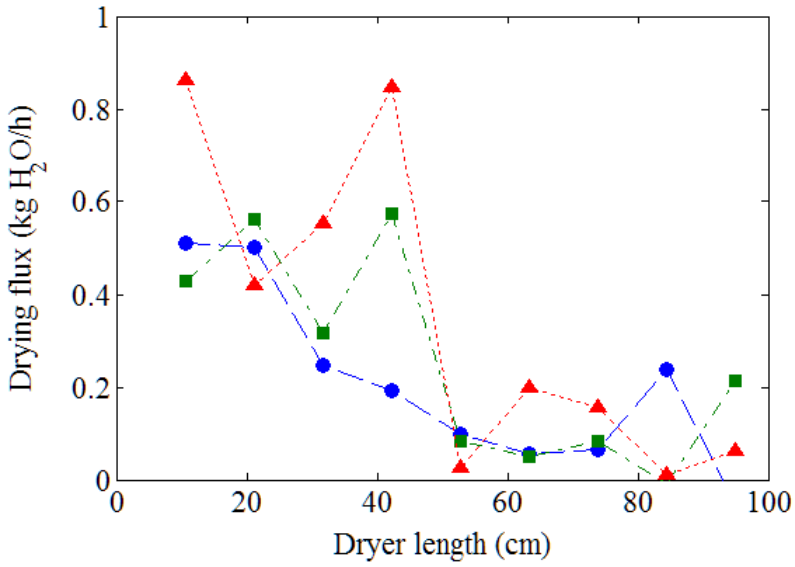

Figure 7: Experimental and simulated water content profiles (left) and drying fluxes profiles (right) for the three experiments

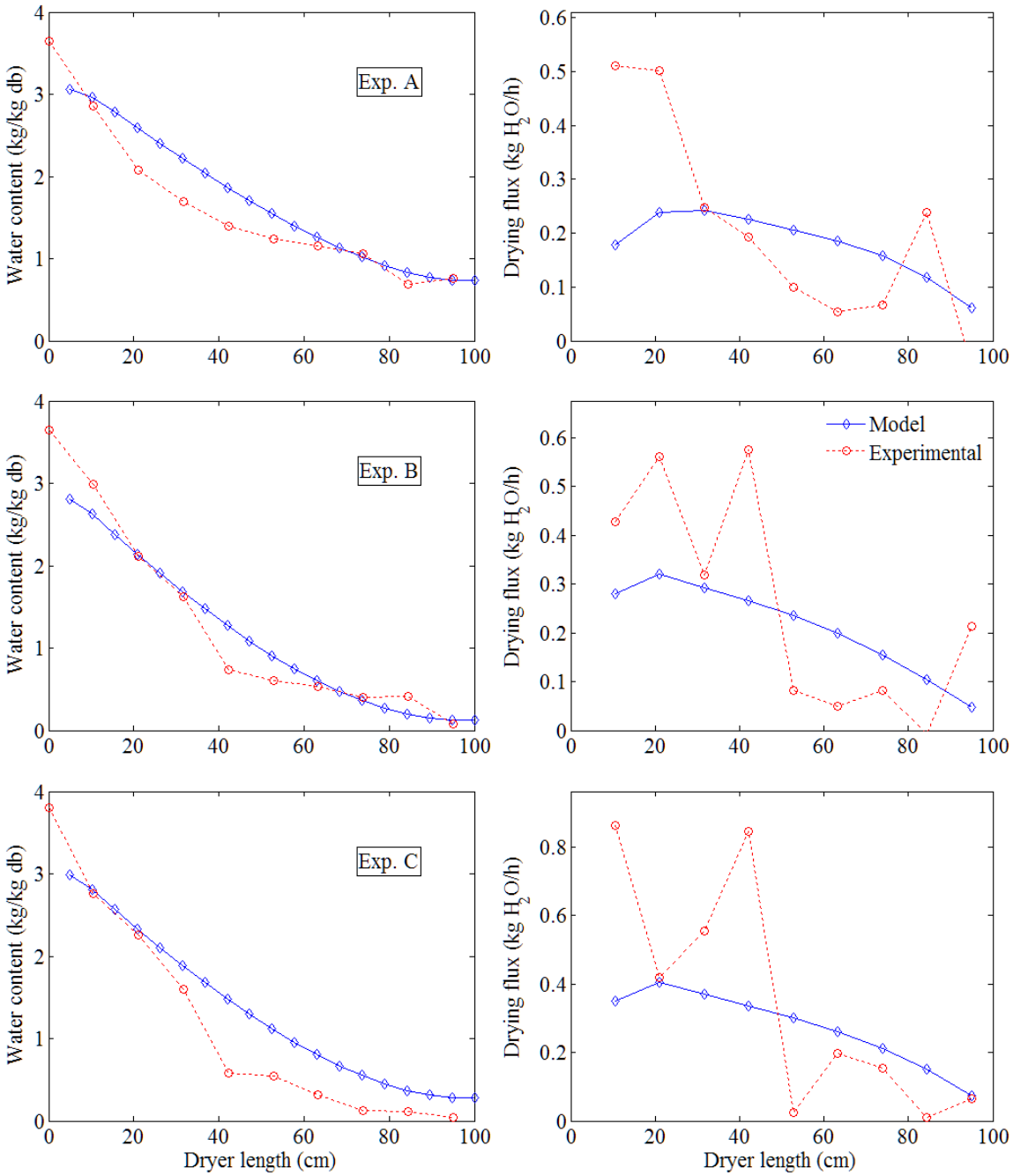

Figure 8: Krischer curve for the three simulations with parameters corresponding to experiments A (O), *B* (□) *and C* (Δ)

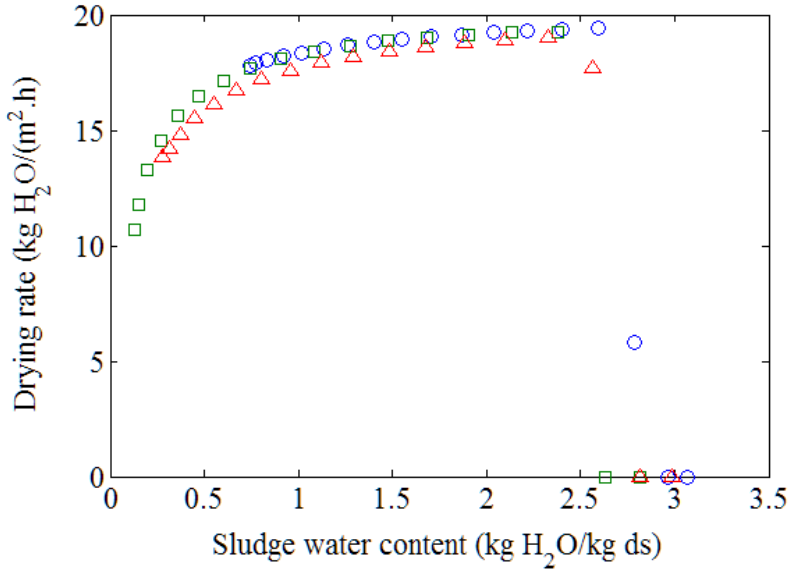

Figure 9: Sludge temperature vs. water content for the three simulations corresponding to experiments A (O), *B* (□) *and C* (Δ)

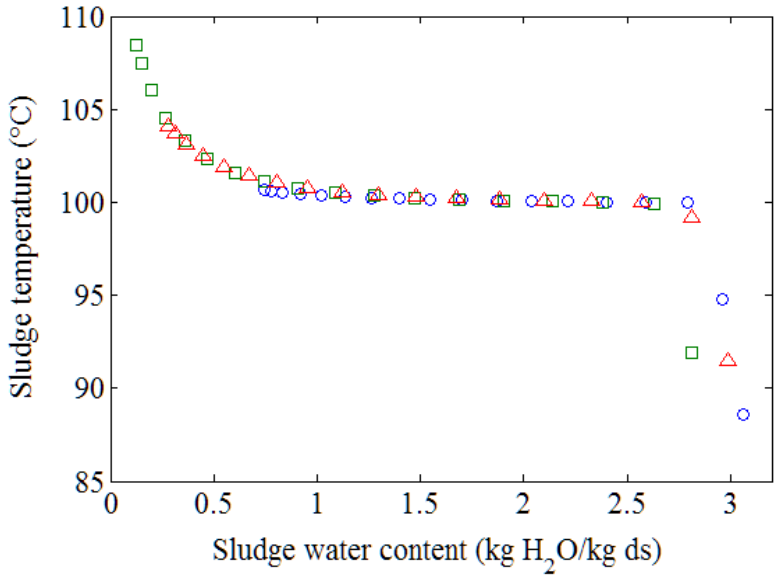

Figure 10: Simulated water content profiles with varying dryer wall temperatures

(140°C: o*; 150°C:* □*; 160°C:* ×*; 170°C:* Δ*; 180°C:* ∇*)*

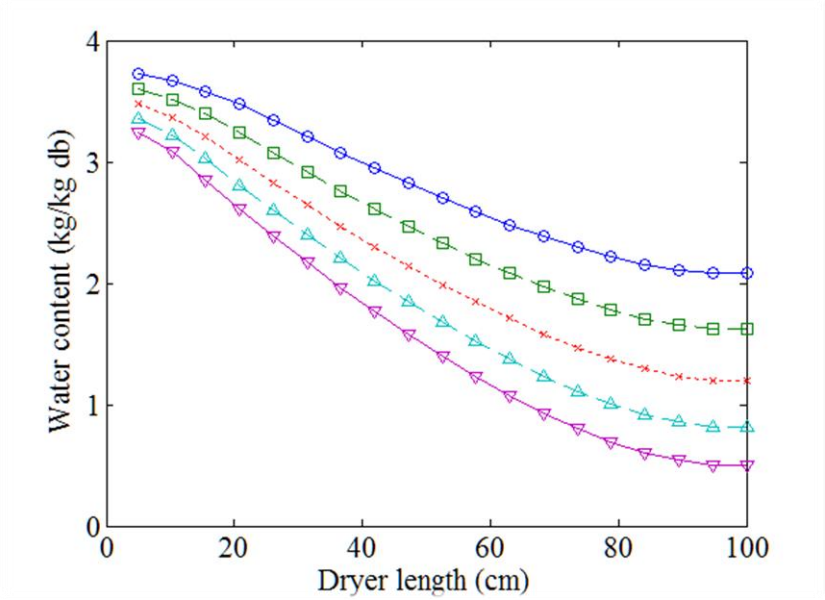

Figure 11: Simulated water content profiles with varying SS inlet flow rates

(3 kg/h: o; 4 kg/h: □; 5 kg/h: ×; 6 kg/h: Δ; 7 kg/h: ∇)

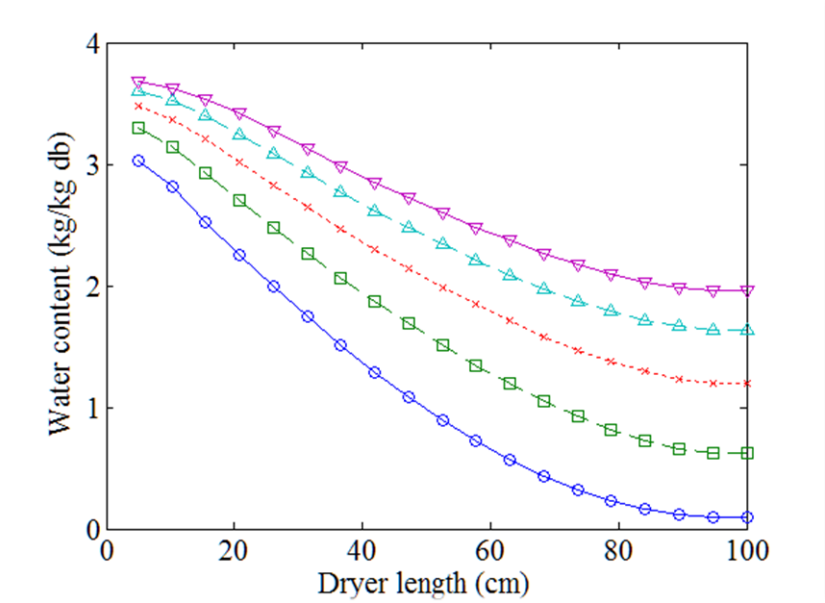

Figure 12: Simulated water content profiles with varying stirring speeds

(10 rpm: o; 20 rpm: □; 30 rpm: ×; 40 rpm: Δ; 50 rpm: ∇)

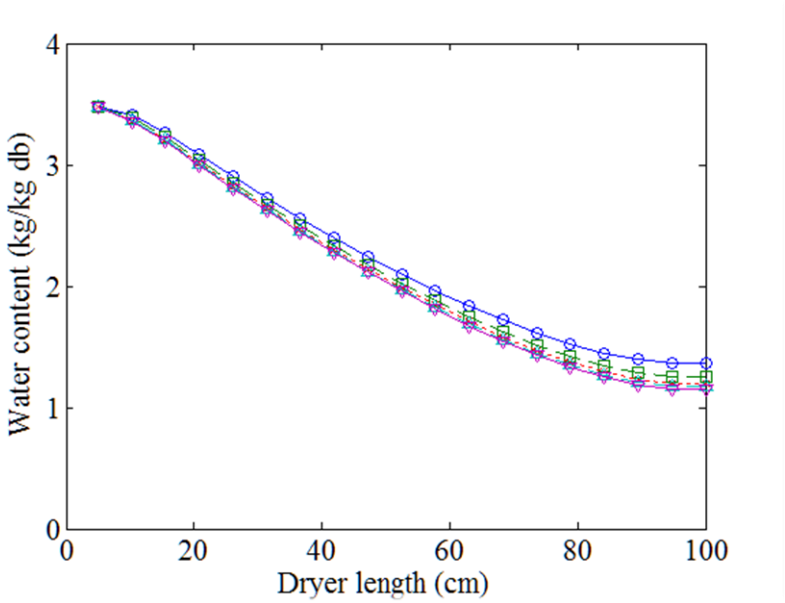

Figure 13: Simulated water content profiles with varying SS initial water contents

(3 kg/kg: o; 3.5 kg/kg: □; 4 kg/kg: ×; 4.5 kg/kg: Δ; 5 kg/kg: ∇)

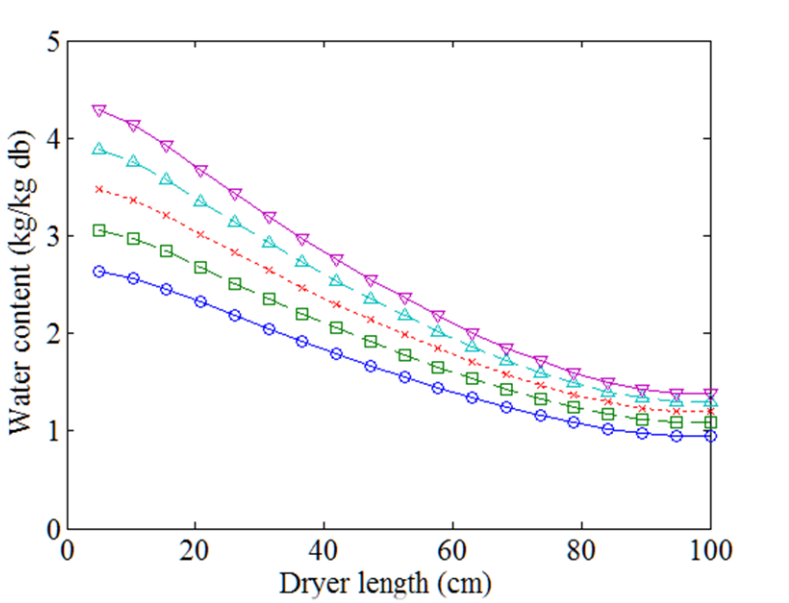

Figure 14: Simulated water content profiles with varying R values

(R = 1: o; R = 2: □; R = 4: ×; R = 8: Δ; R = 12: ∇)

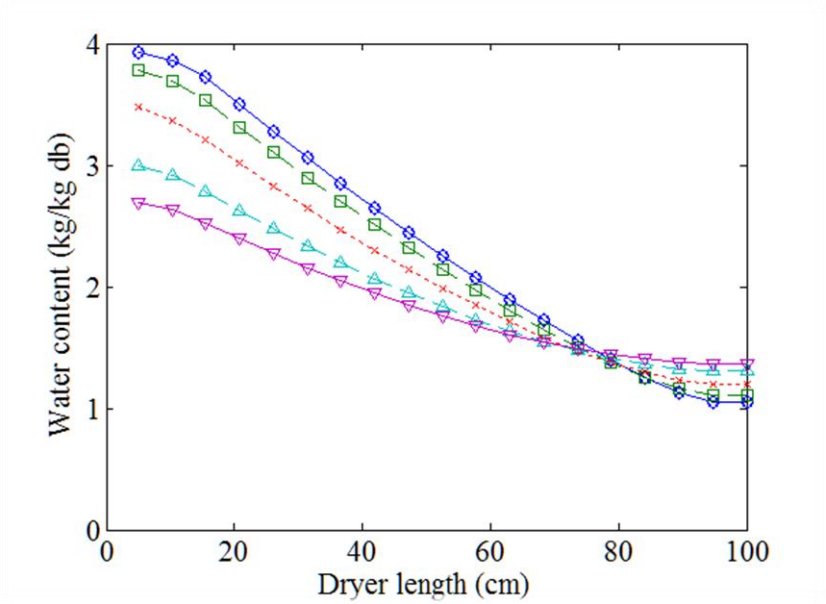
Water content (kg/kg db)
Dryer length (cm)
0
1
2
3
4
0
20
40
60
80
100